Available on CMS information server **CMS IN 2007/XXX**

CMS Internal Note

The content of this note is intended for CMS internal use and distribution only

July 30, 2007

Dijet Ratio from QCD and Contact Interactions

Manoj Jha

University of Delhi, India

Robert M. Harris

Fermilab, Batavia, IL, USA

Marek Zielinski

University of Rochester, Rochester, NY, USA

Abstract

We study the dijet ratio from QCD and contact interaction using CMSSW. We found that the results are similar to Physics TDR II. With only $10pb^{-1}$ of data, CMS will be sensitive to a contact interaction just beyond the present Tevatron limit. We also optimize the η cuts which have been used for calculating the dijet ratio for best sensitivity to contact interactions. The signal sensitivity has been enhanced after optimization of η cuts. For an integrated luminosity of 10 pb^{-1}, 100 pb^{-1}, and 1 fb^{-1}, CMS can expect to exclude at 95% CL a contact interaction scale Λ of $5.3, 8.3$, and 12.5 TeV or discover at 5σ significance a scale Λ of $4.1, 6.8$, and 9.9 TeV, respectively.

1 Introduction

The first limit on the size of atomic nucleus was obtained by Geiger and Marsden in the Rutherford [1] scattering of α particles from nuclei. In an analogous way, we will be able to set a limit on the size of quarks by observing the scattering of the highest energy partons in pp collision at the LHC collider of center-of-mass energies at 14 TeV. In quantum chromodynamics (QCD), parton parton scattering processes are mainly t-channel exchanges and produce dijet angular distributions peaked at small center-of-mass scattering angles; many processes containing new physics are more isotropic. Dijet final states in pp collisions can be produced through quark-quark, quark-gluon, and gluon-gluon interactions. The angular distributions produced by these processes as predicted by theory are similar. Therefore the dijet angular distribution is insensitive to the relative weighting of the individual hard scattering processes thus is insulated from uncertainties in the parton distribution functions (pdf's). Thus the dijet angular distribution provides an excellent test of QCD dynamics and a means of searching for new physics which are beyond the search of present mass scale (Λ) which characterizes the strength of quark substructure binding interactions and the physical size of the composite states. New physics at a scale Λ above the mass of the final state is effectively modelled as a contact interaction. Signals from contact interactions are generic in nature for physics beyond the Standard Model.

This analysis focuses on CMS sensitivity of quark compositeness within the formalism of Eichten et al [2, 3, 4]. An earlier study towards CMS sensitivity to quark contact interactions using ORCA can be found in [5]. In the Lagrangian of Ref. [2, 3, 4], we study the compositeness of left-handed quarks in the left-left isoscalar term

$$L_{qq} = A(g^2/2\Lambda_{LL}^2)\overline{q}_L\gamma^\mu q_L\overline{q}_L\gamma_\mu q_L,$$

where $A = \pm 1$ is the sign of the interference term, Λ_{LL} is the compositeness scale, and the dependence on α_s is contained in the compositeness coupling constant g^2. The model is completely determined by specifying the two parameters A and Λ_{LL}. In this model, all three families of quarks are assumed to be composite, and both signs of the interference term [resulting in constructive (-1) and destructive $(+1)$ interference] are investigated.

1.1 Contact Interaction Searches in Mass

In the presence of contact interaction, we expect an increase in rate relative to QCD at high dijet mass. For example, in Fig 1, we have shown the dijet mass distribution of quark contact interaction for different values of compositeness scale Λ compared to lowest order QCD generated with Pythia [6]. The contact interaction rate increases at higher mass and for smaller the compositeness scale its effect is larger. However, observation of contact interactions in the mass distribution is difficult because there are large systematic uncertainty in both the measurement and the QCD calculation of the cross-section as a function of dijet mass. Moreover, jet energies uncertainties are being multiplied by the steeply falling QCD spectrum to give a large uncertainties in the cross-section. The CDF experiment at Fermilab, Tevatron observed the increase in rate of high jet P_T and dijet mass in comparison to QCD predictions [7]. After those measurements, the dijet mass and jet P_T distributions at the Tevatron were no longer used to search for or constrain contact interactions.

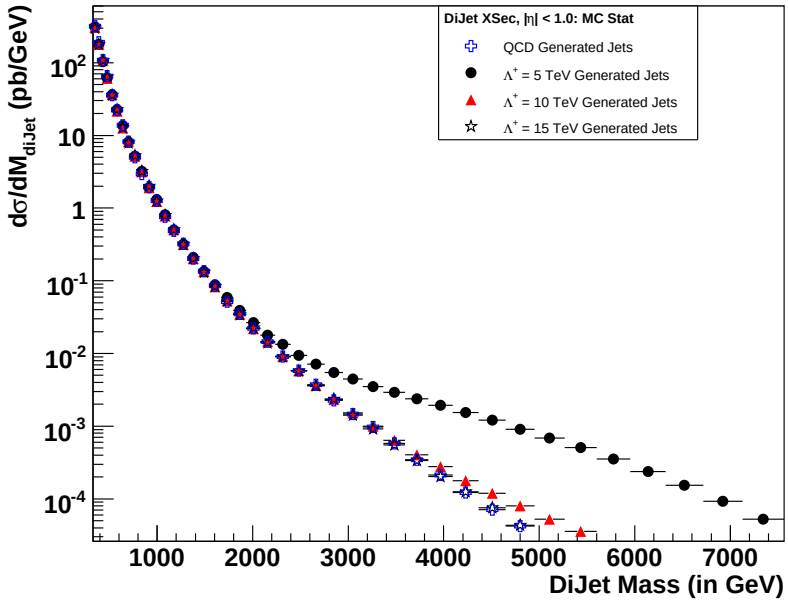

Figure 1: The leading order calculation of the dijet mass distribution from QCD and from QCD plus contact interaction with scales of 3 TeV, 5 TeV, 10 TeV, and 15 TeV.

2 Dijet Ratio

The dijet system consists of the two jets with the high transverse momentum in the event (leading jets). The dijet events are defined as $pp \rightarrow 2$ leading jets $+X$, where X can be anything, including additional jets. The dijet invariant mass is defined as $\sqrt{(E_1+E_2)^2-(\vec{P}_1+\vec{P}_2)^2}$. To characterize the shape of the angular distribution in a mass bin with a single number, we use the variable $R = N(|\eta| < \eta_1)/N(\eta_1 < |\eta| < \eta_2)$, the ratio of the number of dijet events with $|\eta| < \eta_1$ to the number of dijet events with $\eta_1 < |\eta| < \eta_2$. In the flowing discussion, we adopt the values of $\eta_1 = 0.5, \eta_2 = 1.0$ which were used in the original DØ analysis [8]. In section 6, we optimize these values within the CMS barrel region. Fig(2(a), 2(b)) shows the leading order cross-section for QCD and QCD+contact interaction respectively in the central ($|\eta| < \eta_1$) and forward ($\eta_1 < |\eta| < \eta_2$) region. The cross-section for QCD is peaked in the forward region due to t-channel exchange of gluons among point like quarks. In contrast, the cross-section is more in central region for QCD plus contact interaction since they originates from hard interactions than conventional QCD.

Figs 3(a) and 3(b) depict the dijet ratio from leading order calculation from QCD and QCD plus contact interaction at initial parton and particle jet level. There exists a good agreement between dijet ratio distributions at parton and particle level in the low dijet mass region, while a deviation of 5% occurs at higher dijet mass. The lowest order QCD gives a fairly flat dijet ratio around 0.6. For QCD plus contact interaction, the ratio increases with dijet mass and decreases at large mass with increase in compositeness scale.

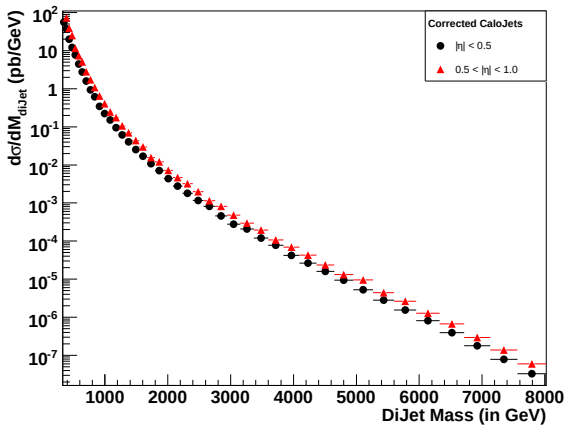

(a) QCD

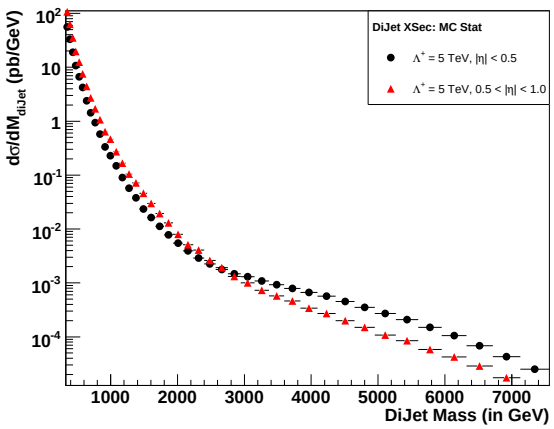

(b) QCD plus contact interaction

Figure 2: A leading order calculation of dijet mass distribution in central and forward region of barrel in CMS for QCD (2(a)) and QCD plus quark contact interaction (2(b)).

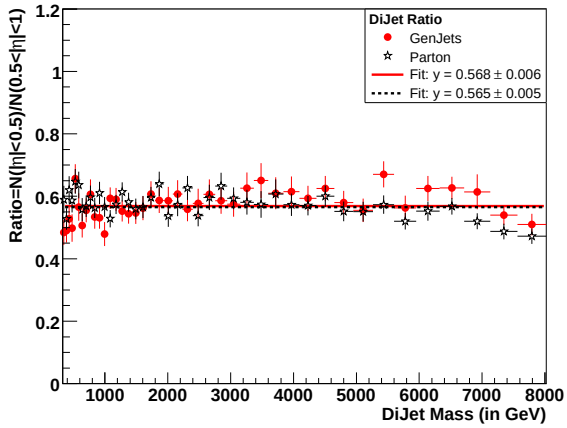

(a) QCD

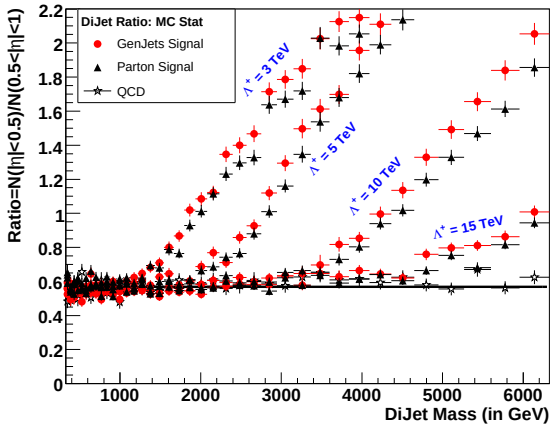

(b) QCD plus contact interaction

Figure 3: The leading order calculation of dijet ratio at parton and particles jet level for QCD (3(a)) and QCD plus contact interaction(3(b)).

3 CMSSW_1_2_0 QCD Samples

This analysis employs Monte Carlo QCD event samples produced for the Software and Detector Performance Validation (SDPV) exercise using CMSSW_1_2_0. The particle-level events were generated with PYTHIA 6.227 using the Tune DWT for Underlying Event parameters [9]. The CMS detector simulation as implemented in CMSSW_1_2_0 based on the GEANT4 package was used to simulate passage of particles through the detector and the energy deposits in the sensitive volumes. All the results which are presented here have been derived from samples without pileup. QCD dijet samples were generated in 21 bins of the momentum transfer in the parton hard-scatter, $\hat{P}_T$, which span the full kinematic range [10]. Each sub-sample has a weight corresponding to the generated cross section per event for that sub-sample. When making the dijet ratio histogram all events from each sub-sample are used along with their corresponding weight and all errors are calculated taking into account the weights.

3.1 Jet Reconstruction

Jet reconstruction is a two-step procedure. In the first step, an arbitrary input collection is treated as a set of Lorentz vectors. Every Lorentz vector satisfying energy and/or E_T requirements is used by the jet clustering algorithm. In the second step, after jet clustering is completed, kinematic information is extracted from objects contributing to the jet, and corresponding values are associated with the jet. We are using Midpoint cone 0.5 algorithm for reconstructing jets at generated (GenJets) and calorimetry (CaloJets) level. Scheme B cell threshold is applied for reconstructing CaloJets. Since jet response is not constant with respect to η, Monte Carlo jet corrections have been applied to CaloJets [11].

In Fig 4, we show the dijet ratio from full CMS detector simulation for jets at generated, calorimetry and corrected calorimetry levels. The dijet ratio from corrected calojets and generated jets are similar at 0.6. The ratio from calojets is higher due to response variation versus η. The jet response in central of barrel is greater than $0.5 < |\eta| < 1.0$ due to expected 1-2$\%$ change in relative jet response in these η regions.

4 Dijet Ratio for Sensitivity Estimates

In Fig 5, we present a prediction of dijet ratio for QCD and QCD plus contact interaction for four values of integrated luminosity. The early period of CMS will correspond to integrated luminosity of 10 pb^{-1} and 100 pb^{-1} while the later phase belongs to 1 fb^{-1} and 10 fb^{-1}. The error bars shown in Fig 5 are the statistical uncertainties expected for four different integrated luminosity values 10 pb^{-1}, 100 pb^{-1}, 1 fb^{-1} and 10 fb^{-1} and jet trigger table proposed in reference [12].

The statistical uncertainties on the dijet ratio in Fig 5 are smooth estimates for the integrated luminosities shown. The calculation of the statistical uncertainties is discussed in [5]. We use Poisson statistics at high dijet mass where few events are expected. For the QCD background, for all four integrated luminosities, the highest mass bin we show in Fig 5 has a mean value of expected events in the numerator of approximately 1.5 events and a mean value of expected events in the denominator of approximately 2.5 events.

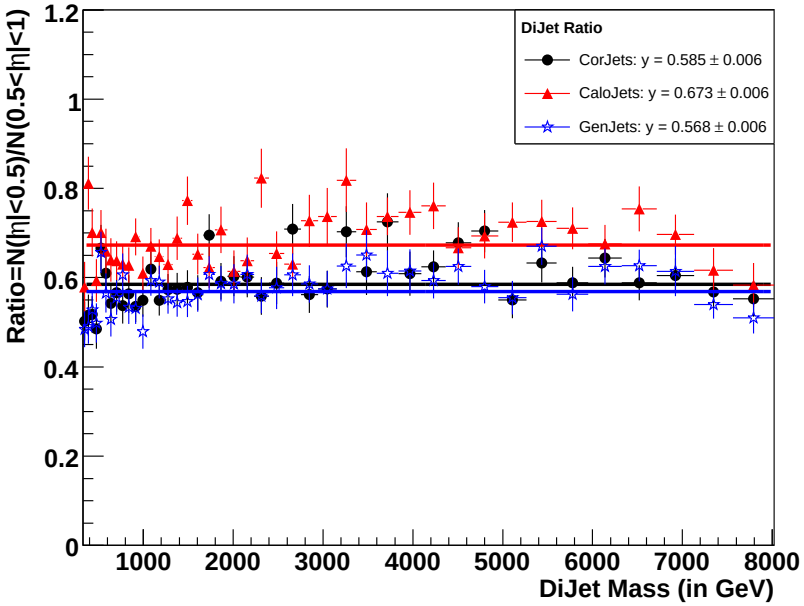

Figure 4: A leading order calculation of dijet ratio from QCD for GenJets, CaloJets, and CorJets.

Comparing the contact interaction signals in Fig 5 to the QCD background and its statistical uncertainty indicates CMS level of sensitivity expect for contact interactions. For 10 pb^{-1}, it will be difficult to discover or exclude $\Lambda = 5$ TeV, which is too close to QCD, but we expect sensitivity to roughly $\Lambda = 3$ TeV at high mass. The last Tevatron limit on compositeness scale is 2.7 TeV at 95% confidence level for integrated luminosity of 100 pb^{-1}. For 100 pb^{-1}, we expect to discover or exclude $\Lambda = 5$ TeV. For 1 fb^{-1}, statistical errors are reduced at high mass, and should be sensitive to roughly $\Lambda = 10$ TeV, since that curve is now at the edge of error bars. For 10 fb^{-1} the statistical errors are reduced again, and we expect sensitivity to $\Lambda = 15$ TeV.

5 Contact Interaction Sensitivity Estimates

To make quantitative estimates of sensitivity to contact interactions, we employ a χ^2 method. In Fig 5, we visually compare QCD plus a contact interaction to QCD alone and its estimated statistical uncertainties for 10 pb^{-1}, 100 pb^{-1} , 1 fb^{-1} and 10 fb^{-1}. In Fig 6, we show the estimated significance for statistical errors only. In this section, we form a χ^2 between QCD plus a contact interaction and QCD alone, and use that χ^2 to estimate the Λ values we expect to be able to exclude at 95% CL and the Λ values we expect to be able to discover at 5σ.

5.1 Sensitivity with Statistical Uncertainties

In Table 1, we show the χ^2 with statistical uncertainties only between QCD plus a contact interaction and QCD alone.

$$\chi^2 = \sum_i \frac{\Delta_i^2}{\sigma_i^2} \tag{1}$$

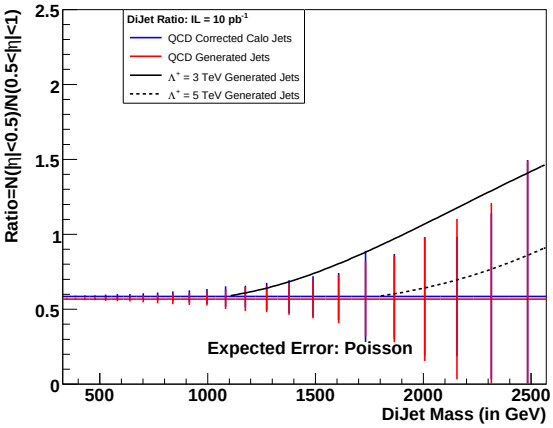

(a) 10 pb^{-1}

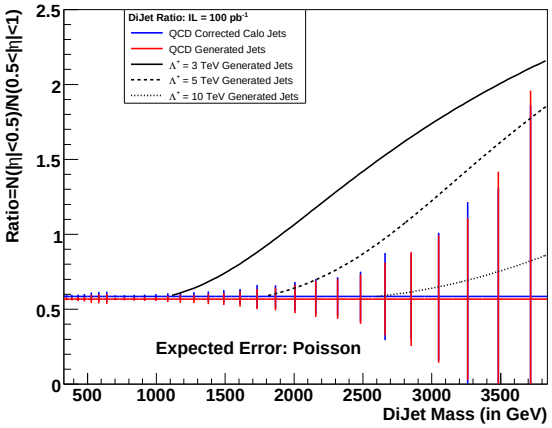

(b) 100 pb^{-1}

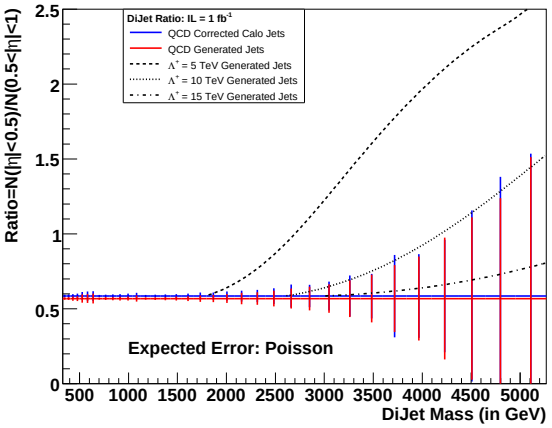

(c) 1 fb^{-1}

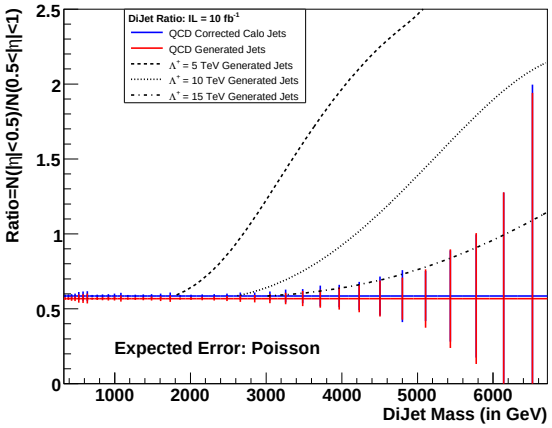

(d) 10 fb^{-1}

Figure 5: Dijet Ratio of QCD is compared with QCD plus a quark contact interaction for early and latter period of CMS.

where for each bin i, Δ_i is the difference between QCD plus a contact interaction and QCD only, and σ_i is the statistical uncertainty on QCD, as shown in Fig 5. Since all our estimates are smooth, without statistical fluctuations in either the background or the signal, the χ^2 tends to zero when the contact interaction scale is very large ($\Lambda \to \infty$) and the signal distribution becomes identical to QCD. This is different than a χ^2 in the presence of actual statistical fluctuations, which is seldom expected to be zero.

Luminosity	$10\ pb^{-1}$				$100\ pb^{-1}$				$1\ fb^{-1}$			
Λ (TeV)	3	5	10	15	3	5	10	15	3	5	10	15
χ^2 (stat)	16.07	0.42	0.002	5.4 e-05	281.2	21.75	0.205	0.036	3236	406.5	10.24	1.135

Table 1: χ^2 between QCD (background) and QCD plus contact interaction (signal).

In Fig 6, we plot the significance versus $1/\Lambda$. As discussed, $1/\Lambda = 0$ corresponds to QCD, no contact interaction signal, and observe a $\chi^2 = 0$ and a significance of 0σ as expected. A 95% CL exclusion corresponds to a significance of 1.96σ for a two sided Gaussian probability for the signal, and this level is shown by a horizontal dotted line in Fig 6. A 5σ discovery level is also shown by a horizontal dotted line in Fig 6. For integrated luminosities of 10 pb^{-1}, 100 pb^{-1}, 1 fb^{-1}, 10 fb^{-1}, we compare the significance for four different values of $\Lambda = 3, 5, 10$, and 15 TeV to these levels. A quadratic function is used to fit to the four points as shown in Fig 6 and is used to find the 95% CL and 5σ values of Λ for 10 pb^{-1} and 100 pb^{-1}. For an integrated luminosity of 1 fb^{-1}, a quartic function has been used for fitting the four points. We found that 95% CL point is below the 15 TeV point so we use the constraint that $\Lambda = \infty$ corresponds to significance of 0σ for calculating the 95% CL and then we fit these points with a quartic function. In Table 2 we show the resulting Λ values for a 95% CL exclusion or 5σ discovery with statistical uncertainties only.

	95% CL Excluded Scale				5σ Discovered Scale			
	$10\ pb^{-1}$	$100\ pb^{-1}$	$1\ fb^{-1}$	$10\ fb^{-1}$	$10\ pb^{-1}$	$100\ pb^{-1}$	$1\ fb^{-1}$	$10\ fb^{-1}$
Λ (TeV)	< 3.8	< 6.8	< 9.1	< 18.0	< 2.8	< 4.9	< 8.6	< 13.8

Table 2: Statistical senstivity to contact interactions with 10 pb^{-1}, 100 pb^{-1}, 1 fb^{-1}, 10 fb^{-1}. Estimates include ONLY statistical uncertainties.

6 Optimization of η cuts within the Barrel

Till now, we have used the η cuts from Tevatron for calculating the dijet ratio from QCD and QCD plus contact interaction. Here, we optimize the η cut for achieving the maximum sensitivity of the signal with respect to the background within the barrel region of the CMS calorimeter.

Table 3 shows the χ^2 values as function of inner and outer η cut. We have considered the outer η cut (first row) from 0.9 upto 1.3 while the inner eta cut (first colum) starts from 0.3 upto 0.9 in steps of 0.1. The η cut of 1.3 corresponds to maximum value to stay within barrel. This value also corresponds to the optimal choice of eta cut for dijet resonances searches [13]. The optimized η cut will corresponds to maximum sensitivity, i.e., maximum χ^2.

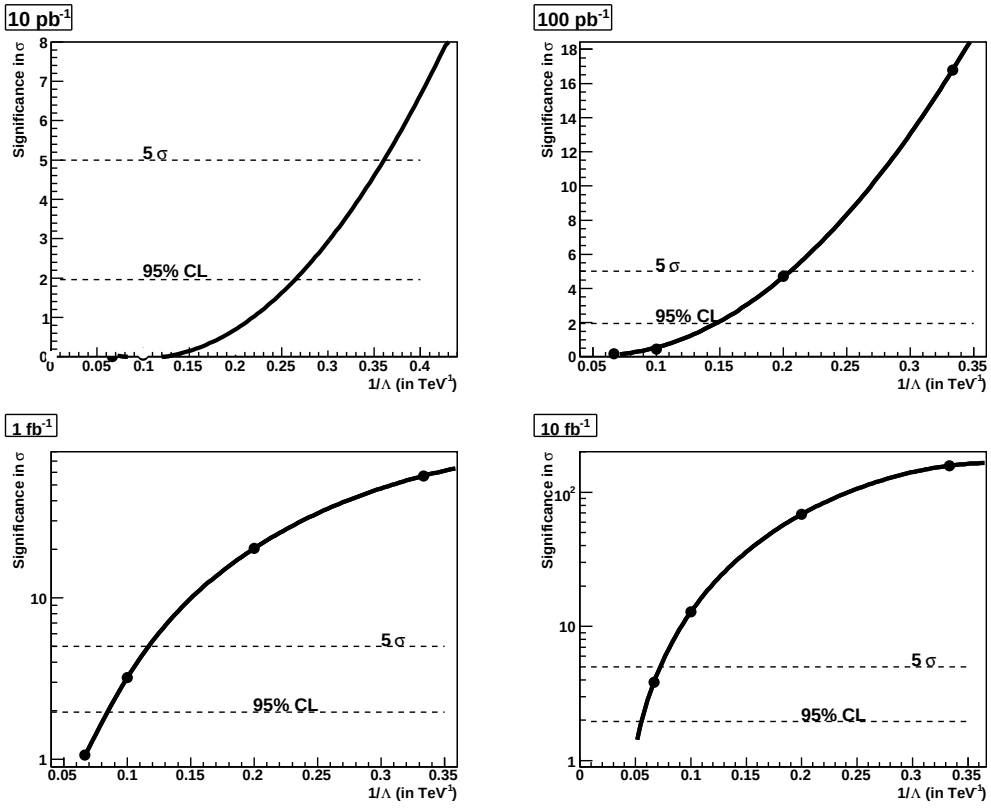

Figure 6: Significance with statistical uncertainties only of the difference between QCD and QCD plus contact interaction for integrated luminosities of 10 pb^{-1}, 100 pb^{-1}, 1 fb^{-1}, and 10 fb^{-1}. The significance is plotted vs $1/\Lambda$ and fitted with a smooth function. Horizontal line show the 5σ and 95% CL levels.

	0.9	1.0	1.1	1.2	1.3
0.3	4.6	9.8	19.8	32.0	44.9
0.4	7.0	16.6	34.5	56.3	80.6
0.5	9.1	20.4	55.1	91.6	128.9
0.6	9.1	21.9	63.6	129.6	182.3
0.7	4.2	13.7	54.8	116.1	199.9
0.8		12.7	50.1	101.8	170.8
0.9			35.7	86.4	145.3

Table 3: χ^2 between QCD and QCD plus contact interaction as function of inner (first column) and outer (first row) η cuts. Consider only the statistical error.

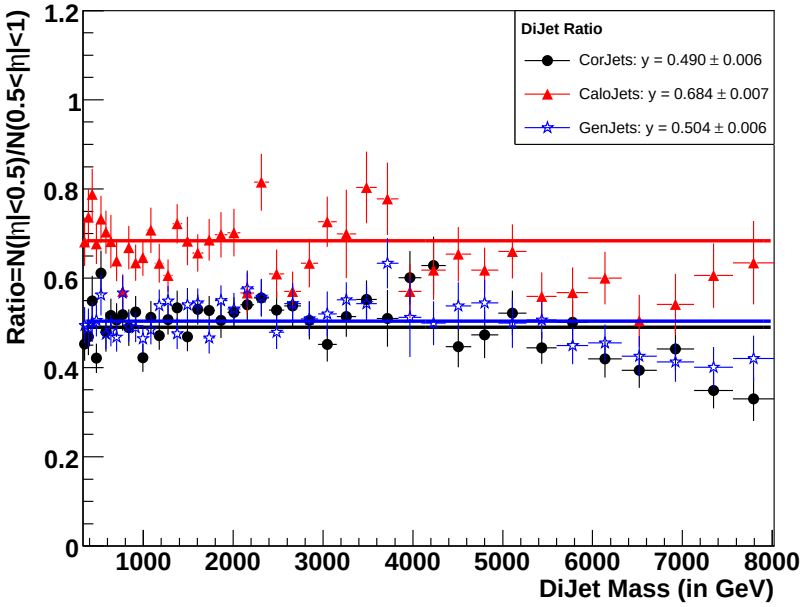

Figure 7: A leading order calculation of dijet ratio from QCD for GenJets, CaloJets, and CorJets for optimized η cuts.

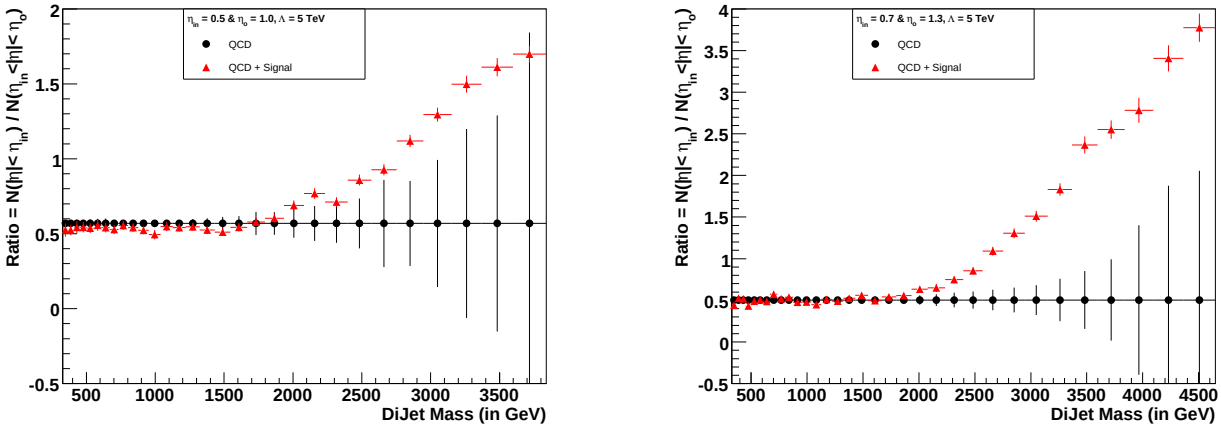

(a) η cut from Tevatron

(b) Optimized η cut

Figure 8: Dijet ratio for η cut from Tevatron and optimzed η cuts.

The maximum value of χ^2 is 199.9 and it corresponds to η outer (η_o) and η inner (η_i) of 1.3 and 0.7 respectively.

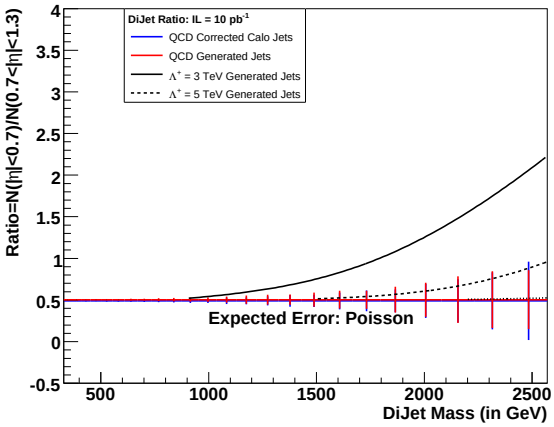

(a) 10 pb^{-1}

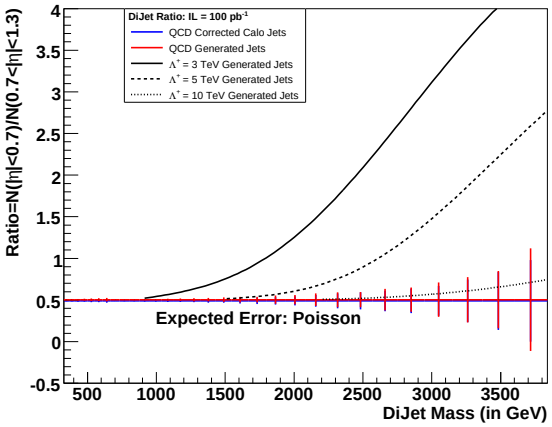

(b) 100 pb^{-1}

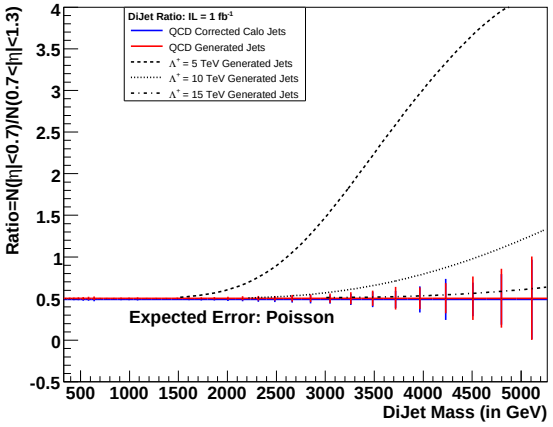

(c) 1 fb^{-1}

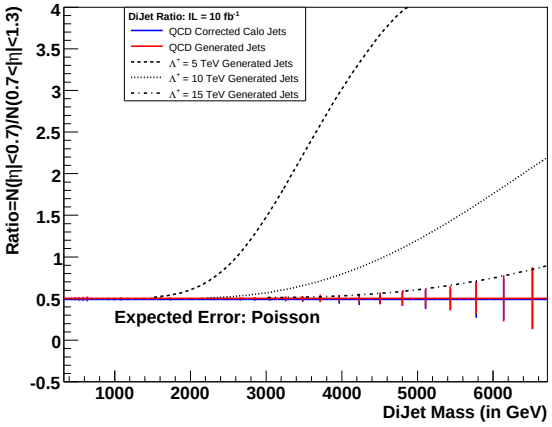

(d) 10 fb^{-1}

Figure 9: Dijet Ratio of QCD is compared with QCD plus a quark contact interaction for early and latter period of CMS for optimized η cuts.

In Fig 7, we show the dijet ratio from full CMS detector simulation for jets at generated, calorimetry and corrected calorimetry levels for optimized η cuts. The dijet ratio from corrected calojets and generated jets are similar at 0.5. Fig 8 shows the dijet ratio from QCD and QCD plus contact interaction for η cuts from Tevatron and with the optimized η cut. The signal sensitivity for optimized η cut has been enhanced with respect to the η cut from Tevatron. In Fig 9, we estimated the dijet ratio for QCD and QCD plus contact interaction from optimized η cut for four values of integrated luminosity. The sensitivity to signal for optimized η cut has been enhanced than the earlier case (Fig 5). In Fig 10, we plot the significance versus $1/\Lambda$. In Table 4, we have shown the χ^2 with statistical uncertainties only between QCD and QCD plus contact interaction for the optimized η cut.

In Table 5, we show the values of Λ that corresponds to 95% CL exclusion and 5σ discovery scales.

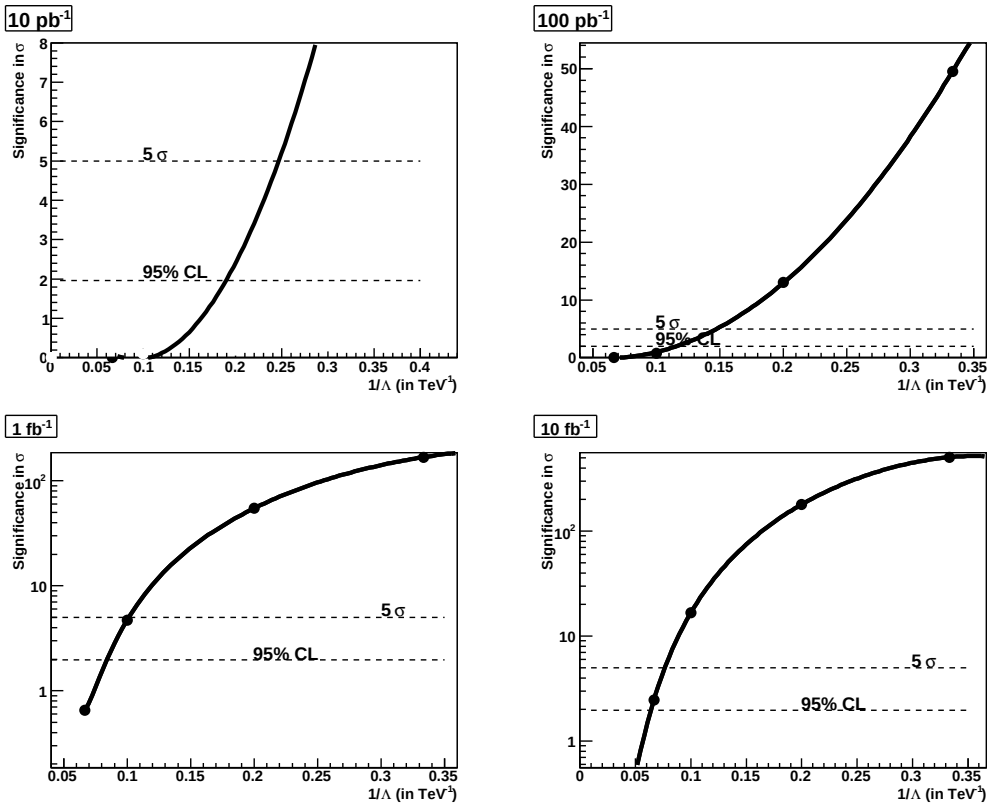

Figure 10: Significance with statistical uncertainties only of the difference between QCD and QCD plus contact interaction for integrated luminosities of 10 pb^{-1}, 100 pb^{-1}, 1 fb^{-1}, and 10 fb^{-1} for optimized η cuts. The significance is plotted vs $1/\Lambda$ and fitted with a smooth function. Horizontal line show the 5σ and 95% CL levels.

Luminosity	10 pb^{-1}				100 pb^{-1}				1 fb^{-1}			
Λ (TeV)	3	5	10	15	3	5	10	15	3	5	10	15
χ^2 (stat)	151	5.6	0.01	0.0001	2450	169.1	0.5594	0.0054	2.83e+04	3005	22.32	0.4271

Table 4: χ^2 between QCD (background) and QCD plus contact interaction (signal) for optimized η cuts.

	95% CL Excluded Scale				5σ Discovered Scale			
	10 pb^{-1}	100 pb^{-1}	1 fb^{-1}	10 fb^{-1}	10 pb^{-1}	100 pb^{-1}	1 fb^{-1}	10 fb^{-1}
Λ (TeV)	< 5.3	< 8.6	< 12.2	< 15.6	< 4.1	< 6.8	< 9.9	< 13.1

Table 5: Statistical senstivity to contact interactions with 10 pb^{-1}, 100 pb^{-1}, 1 fb^{-1}, and 10 fb^{-1} for optimized η cut. Estimates include ONLY statistical uncertainties.

7 Conclusion

We study the dijet ratio from QCD and contact interaction using CMSSW. We found that the results are similar to Physics TDR II [14]. With only $10pb^{-1}$ of data, CMS will be sensitive to a contact interaction just beyond the present Tevatron limit. We also optimize the η cuts which have been used for calculating the dijet ratio for best sensitivity to contact interactions. The signal sensitivity has been enhanced after optimization of η cuts. For an integrated luminosity of 10 pb^{-1}, 100 pb^{-1}, and 1 fb^{-1}, CMS can expect to exclude at 95% CL a contact interaction scale Λ of $5.3, 8.3$, and 12.5 TeV or discover at 5σ significance a scale Λ of $4.1, 6.8$, and 9.9 TeV, respectively.

Contact interaction signal are generic signals for new physics. These signals are generally observed first before any exchanged particles are directly seen. This analysis shows that dijets at CMS can provide an early signal of physics beyond the Standard Model.

References

[1] **Cambridge University Press, Cambridge, England, 1930**, E. Rutherford, J. Chadwick, and C. D. Ellis, *"Radiations from Radioactive Substances"*.

[2] **Phys. Rev. Lett. 50, 811 (1983)**, E. Eichten, K. Lane, and M. E. Peskin, *"New Tests for Quark and Lepton Substructure"*.

[3] **Rev. Mod. Phys. 56, 579 (1984), 58, 1065 (1986)**, E. Eichten, I. Hinchiliffe, K. Lane, and C. Quigg, *"Super-collider physics"*.

[4] **hep-ph/9605257**, K. Lane, *"Electroweak and Flavor Dynamics at Hadron Colliders"*.

[5] **CMS Note - 2006/071**, Selda Esen and Robert M. Harris, *"CMS Sensitivity to Quark Contact Interactions using Dijets"*.

[6] **Phys. Commun. 82, 74 (1994)**, T. Sjöstrand *"PYTHIA"*.

[7] **Phys. Rev. Lett. 77, 438 (1996), hep-ex/9601008**, F. Abe et al. *"Inclusive Jet Cross Section in pp Collisions at $\sqrt{s} = 1.8$ TeV"*.

[8] **Phys. Rev. Lett. 82, 2457 (1999)**, B. Abbott et al. *"Dijet Mass Spectrum and a Search for Quark Compositeness in $\bar{p}p$ Collisions at $\sqrt{s} = 1.8$ TeV"*.

[9] **CMS-Note - 2006/067**, D. Acosta, et al., *"The Underlying Event at LHC"*.

[10] http://www.uscms.org/LPC/lpc-jetmet/edmData/edmData.html.

[11] **CMS IN - 2007/XXX**, M. Vazquez Acosta, et al., *"Jet and MET Performance in CMSSW_1_2_0."*.

[12] **CMS Note - 2006/069**, Selda Esen, Robert M. Harris, *"Jet Triggers and Dijet Mass."*.

[13] http://indico.cern.ch/getFile.py/access?contribId=3&resId=1&materialId=slides&confId=15403.

[14] **J. Phys. G: Nucl. Part. Phys. 34 995-1579** CMS Collaboration 2007, *CMS Technical Design Report, Volume II: Physics Performance*